Computational Materials Science 91 (2014) 266–273

Contents lists available at ScienceDirect

Computational Materials Science

journal homepage: www.elsevier.com/locate/commatsci

Topological design of microstructures of multi-phase materials for maximum stiffness or thermal conductivity

A. Radman, X. Huang *, Y.M. Xie

Centre for Innovative Structures and Materials, School of Civil, Environmental and Chemical Engineering, RMIT University, GPO Box 2476, Melbourne 3001, Australia

ARTICLE INFO

Article history:
Received 28 December 2013
Received in revised form 26 April 2014
Accepted 29 April 2014
Available online 27 May 2014

Keywords:
Topology optimization
Bulk modulus
Shear modulus
Thermal conductivity
Homogenization

ABSTRACT

This paper introduces an alternative approach for the topological design of microstructures of materials that are composed of three or more constituent phases. It is assumed that the materials are made up of periodic microstructures. Bi-directional Evolutionary Structural Optimization (BESO) methodology is applied for designing materials' microstructures with maximum bulk modulus, shear modulus or thermal conductivity. Constituent phases are divided into groups and sensitivity analyses are performed in order to estimate their effects on the variation of the objective function. Changing the elemental properties in the finite element model of the microstructure is performed based on this sensitivity analyses and by imposing volume constraints on the constituent phases. Numerical examples are presented to demonstrate the effectiveness of the algorithm in terms of identification of the phases' boundaries and convergence speed. The proposed approach could potentially be used to design multiphase materials for functional properties other than stiffness and thermal conductivity.

1. Introduction

In comparison with cellular materials that are composed of one solid phase and a void phase, composites of two or more materials are more advantageous and attractive for practical applications. One of the reasons is that by combining different constituent phases, a wider range of properties could be achieved which are not attainable by individual constituent phases. In addition, multi-functional multifunctional composites more often than not consist of two or more constituent phases [1].

It is known that the physical properties of composites can be altered by changing the composition and/or microstructural topology of the constituent phases. To find the best spatial distribution of the constituent phases within the microstructure of a composite, structural topology optimization methodology can be applied [2,3]. Here, the aim is to solve the inverse problem of finding microstructures with desired functional properties [2]. Different topology optimization techniques offer advantages and disadvantages in terms of computational cost and efficiency, quality of generated microstructures, robustness, and the level of effort for implementation as a computational post-processing procedure, to name few.

In optimization of microstructures for multi-phase materials, it is desirable to represent the topology of the constituent phases by continuous interface functions. The level-set topology optimization method [4] can provide such sharp interfaces between different constituent phases. For this purpose, the approach requires the definition of higher-dimensional functions to represent the boundaries of constituent phases which is mathematically complicated [5]. In addition special attention must be paid to the splitting of phases. The level-set method is generally devised to describe the propagation of interfaces with a defined speed function; therefore, new phase regions within existing shapes and away from the boundaries cannot be initiated without additional schemes [6,7]. Because of the mathematical complications, in general the approach has not reached the stage of regular application for the design of composites with multiple phases.

Homogenization method [8] has also been used for topology optimization of materials' microstructures in a number of studies [9,10]. In these studies the materials' microstructures are considered as a combination of even much smaller microstructures. These latter microstructures are introduced with different material models such as square unit cells with rectangular void or rank layered materials and their properties are controlled by their geometrical parameters. The geometrical parameters are defined as design variables. The objective of optimization is to find their optimal values (for example the sizes and orientation of the void regions in square unit cells). Except for the issue of existence of solutions [11], these types of topology optimization require performing multi-scale analysis [10] which is costly. In addition, in the case of multiphase materials,

* Corresponding author. Tel.: +61 3 99253320; fax: +61 3 96390138.
E-mail address: huang.xiaodong@rmit.edu.au (X. Huang).

http://dx.doi.org/10.1016/j.commatsci.2014.04.064
0927-0256/

the generated ranked laminates have zero shear stiffness in one direction, which makes the solutions unstable [12]. Besides, the optimal solutions usually have high manufacturing costs since there are infinitesimal cavities in the microstructures [12].

Inspired by the homogenization method, Solid Isotropic Material with Penalization (SIMP) has been proposed [8]. It has also been tailored for the design of periodic microstructures for composites with two material phases and a void phase [13,14]. The key point in these studies is the introduction of three design variables (x_{i1}, x_{i2}, x_{i3}) for each element that corresponds to three constituent phases. By defining an artificial mixing function, local material properties are correlated with the design variables. This assumption is only valid if the design variables take their extreme values (for example $x_{i1} = 1$ and x_{i2}, $x_{i3} = 0$, which means that the element is filled with constituent phase 1). To circumvent the numerical instabilities associated with utilizing discrete design variables, the SIMP uses a relaxation method in which the design variables are freed to take any value between 0 and 1 [15]. Such an approach leads to intermediate densities in the final topology. In the SIMP approach, it is tried to eliminate the intermediate densities through penalization in the final solution. However, increasing the penalty exponent not only cannot solve the problem completely, but also may result in difficulties in convergence of the solution [16–18]. In comparison with cellular microstructures designed with single material phase, in topology optimization of multi-phase materials the SIMP usually causes more difficulty in interpretation and identification of the boundaries between constituent phases [19]. Several approaches have been proposed to tackle this issue in literature; Heaviside projection algorithm [20], nonlinear diffusion techniques [21] and the phase field approach based on Cahn–Hilliard model [19] are some of the these methods. Nevertheless, these methods add additional computational cost to the optimization procedure.

Recently, the BESO approach has been developed for stiffness optimization of macro-structures with multiple materials [22,23]. Although the generated structures are topologically similar to the results of the SIMP approach, it has been shown that the procedure is independent of the selection of penalization factor and provides clearer boundaries between different materials. Better convergence of the procedure together with high computational efficiency and more importantly, the capability of the BESO in separating the constituent phases, has made it a more promising tool for topology optimization of multi-phase composite structures.

In this paper, the BESO methodology will be extended into the design of composite materials with three or more non-zero constituent phases. It is assumed that the material is composed of periodic base cells (PBC) and the relationship between material's properties at the macroscopic level and microstructure at the microscopic level is established through the homogenization theory [24,25]. The objective function is defined to achieve materials with maximum bulk modulus, shear modulus or thermal conductivity. The constituent phases are categorized into some groups and sensitivity analyses are performed to assess the contribution of elements within each group to the variation of the objective function. The material type of each element is determined based on these sensitivity numbers and by imposing the volume constraints. To tackle the numerical issues, the filtering is conducted within the elements of each group. Finally, some 2D and 3D numerical examples are presented.

2. Methodology

2.1. Problem statement

The stiffness of a composite material can be described by its bulk or shear modulus of elasticity. Similarly thermal conductivity indicates the behavior of materials in transferring heat. In the stiffness optimization problems, it is assumed that the composite material consists of N constituent phases with equal Poisson's ratios and Young's moduli which are ordered descending (that is: $E^1 > E^2 > \ldots > E^N$). Likewise in the conductivity problems, it is assumed that the thermal conductivities of constituent phases are ordered as $\kappa^1 > \kappa^2 > \ldots > \kappa^N$.

Moreover, it is assumed that the microstructure of composites is represented by a PBC which is discretized into finite elements. The optimization problem statement for attaining a periodic microstructure for composite with maximum bulk modulus, shear modulus or thermal conductivity and with constraints on volume fraction of each constituent phase can be expressed as:

$$\text{Maximize} \quad f(x_{ij}) = K, G \text{ or } \kappa_c$$

$$\text{Subject to}: \quad V^{j*} = \sum_{i=1}^{M} x_{ij} V_i - \sum_{m=1}^{j-1} V^{m*} \tag{1}$$

$$x_{ij} = x_{\min} \text{ or } 1$$

where K, G or κ_c are the bulk modulus, shear modulus or thermal conductivity of composite; M is the total number of elements within the finite element model of the PBC; i and j denote the number of the finite element in the PBC and the number of the constituent phase, respectively. V_i and V^{j*} denote the volume of element i and the prescribed volume of the jth constituent phase. x_{ij} is the design variable which indicates the density of the ith element for the jth material phase and is expressed by:

$$x_{ij} = \begin{cases} 1 & \text{if} \quad E \geq E^j \text{ or } (\kappa > \kappa^j) \\ x_{\min} & \text{otherwise} \end{cases} \tag{2}$$

where E and κ denotes the Young's modulus and thermal conductivity of the ith element and $x_{\min}$ is a very small value (e.g. 0.001). x_{ij} is equal to 1 when the element is filled with material phase j or the constituent phases with larger stiffness/thermal conductivity and $x_{ij} = x_{\min}$ otherwise. As a result, the term $\sum_{i=1}^{M} x_{ij} V_i$ in Eq. (1) denotes the volume summation of the jth phase and stiffer phases ($j+1,\ldots,M$); the volume constraint in Eq. (1) means that the volume of the jth phase should be equal to the prescribed value, V^{j*}.

The physical property of the ith element is interpolated between two neighboring phases using a power-law scheme. For instance, the elemental elasticity matrix $\boldsymbol{D}$ can be interpolated as [22]:

$$\boldsymbol{D}(x_{ij}) = x_{ij}^p \boldsymbol{D}^j + (1 - x_{ij}^p) \boldsymbol{D}^{j+1} \tag{3}$$

in which the subscripts j and $j+1$ indicate the phase numbers and p is the penalty exponent which is usually equal to 3. Similarly the thermal conductivity of the ith element can be interpolated between two neighboring phases as:

$$\boldsymbol{\kappa} = x_{ij}^p \boldsymbol{\kappa}^j + (1 - x_{ij}^p) \boldsymbol{\kappa}^{j+1} \tag{4}$$

2.2. Homogenization theory and sensitivity analysis

For topology optimization of material's microstructures, it is necessary to calculate the macroscopic properties of the composite based on the distribution of constituent phases within its microstructure. If a heterogeneous composite possesses certain types of regularity at the microscale, its properties can be estimated by modeling the PBC with the help of the homogenization theory [24,25]. For example the homogenized elasticity matrix of materials with repeating (periodic) microstructures is expressed as:

$$\boldsymbol{D}^H(x_{ij},\boldsymbol{u}) = \frac{1}{|Y|}\int_Y \boldsymbol{D}(x_{ij})(\mathbf{I}-\boldsymbol{B}\boldsymbol{u})dY \tag{5}$$

where $\boldsymbol{u}$ denotes the displacement fields resulted from imposing uniform strain fields on the base cell (for instance, in 2D problems the uniform strain fields are defined as $\varepsilon_1^0 = [1\ \ 0\ \ 0]^T$, $\varepsilon_2^0 = [0\ \ 1\ \ 0]^T$ and $\varepsilon_3^0 = [0\ \ 0\ \ 1]^T$); $|Y|$ is the total area or volume of the PBC and $\boldsymbol{B}$ is the strain–displacement matrix. The derivation of $\boldsymbol{D}^H$ with respect to changes in design variables x_{ij}, can be expressed as [26]:

$$\frac{\partial \boldsymbol{D}^H}{\partial x_{ij}} = \frac{1}{|Y|}\int_Y (\mathbf{I}-\boldsymbol{B}\boldsymbol{u})^T \frac{\partial \boldsymbol{D}}{\partial x_{ij}}(\mathbf{I}-\boldsymbol{B}\boldsymbol{u})dY \tag{6}$$

Eq. (6) indicates the variation of the stiffness (objective function) with respect to the change in the design variable and is used for calculation of the sensitivity of elements. It should be noted that, different from the microstructural design with two phases, there are $N-1$ groups of sensitivity numbers for the design of multi-phase materials.

The matrix of homogenized thermal conductivity ($\boldsymbol{\kappa}^H$) can be calculated as

$$\boldsymbol{\kappa}^H(x_{ij},\boldsymbol{\mu}) = \frac{1}{|Y|}\int_Y \boldsymbol{\kappa}(x_{ij})(\mathbf{I}-\boldsymbol{\mu})dY \tag{7}$$

in which $\boldsymbol{\mu}$ is the induced temperature field resulting from finite element analysis of the base cell under the periodical boundary conditions and uniform heat flux (e.g. $\{1,\ 0\}^T$ and $\{0,\ 1\}^T$ in 2D cases). The sensitivity of the homogenized thermal conductivity with respect to the design variables x_{ij} can be expressed as [18,25]:

$$\frac{\partial \boldsymbol{\kappa}^H}{\partial x_{ij}} = \frac{1}{|Y|}\int_Y (\mathbf{I}-\boldsymbol{\mu})^T \frac{\partial \boldsymbol{\kappa}}{\partial x_{ij}}(\mathbf{I}-\boldsymbol{\mu})dY \tag{8}$$

2.3. BESO method

Since the design variables are either $x_{\min}$ or 1, the optimality criteria can be described as that the constituent phase j, and those phases that have larger Young's modulus or thermal conductivities than j, always have higher sensitivities than that of the rest constituent phases. With this assumption, a simple BESO scheme can be devised to update the design variable x_{ij} by changing from 1 to $x_{\min}$ for elements with lower sensitivity numbers and from $x_{\min}$ to 1 for elements with higher sensitivity numbers.

When the material's microstructure is composed of N ordered constituent phases, they can be divided into $N-1$ ordered groups and $N-1$ series of sensitivity numbers are calculated for these groups [22]. For instance, when the composite's microstructure is composed of three material phases, BESO starts from a finite element model with nearly all elements with material 1. After the finite element analysis, all elements are ranked in descending order according to their sensitivity numbers and elements with lower sensitivity numbers are turned into material 2 by satisfying the target volume of material 2. The target volume of material 2 is defined by introducing an evolution rate (ER) as:

$$V^2_{(k+1)} = \min\left(V^2_{(k)}(1+ER), V^{2*}\right) \tag{9}$$

where subscript in the parenthesis indicates the iteration number. The transition between materials 1 and 2 is performed based on the sensitivity number α_{i1}. For example, in the case where the objective function is defined to maximize the shear modulus in 2D problems, the sensitivity number of element i (α_{i1}) is defined with the following equation by using Eqs. (3) and (6):

$$\alpha_{i1} = \begin{cases} (1-\varepsilon_{i3})^2(D^1_{33}-D^2_{33}) & \text{for material 1} \\ px^{p-1}_{\min}(1-\varepsilon_{i33})^2(D^1_{33}-D^2_{33}) & \text{otherwise} \end{cases} \tag{10a}$$

in which ε_{i3} is the shear strain induced in element i. Superscripts on D indicate the constituent phases and the subscript 33 indicates the corresponding element of the stiffness matrix; p is the penalty exponent which is usually equal to 3. The gradual addition of material 2 continues until its volume reaches to the prescribed value. At this stage, the total volume of material 2 is kept constant but its distribution within the PBC is allowed to change. Then the volume of material 3 is allowed to gradually increase. The transition between elements with materials 2 to 3 is performed by introducing a second series of sensitivity numbers (α_{i2}) and ranking elements based on this sensitivity numbers. For the above example α_{i2} is defined as:

$$\alpha_{i2} = \begin{cases} (1-\varepsilon_{i3})^2(D^2_{33}-D^3_{33}) & \text{for materials 1 and 2} \\ px^{p-1}_{\min}(1-\varepsilon_{i33})^2(D^2_{33}-D^3_{33}) & \text{otherwise} \end{cases} \tag{10b}$$

where $D^2_{33} > D^3_{33}$. It can be seen that the transition between materials 1 and 3 may happen indirectly (by changing into material 2 in the first place). However, they are not interchanged directly; therefore there is no need for calculation of a new series of sensitivity numbers between materials 1 and 3. The procedure of increasing the number of elements with material 3 continues until the volume of material 3 satisfies the prescribed value. If there are more than 3 constituent phases, similar procedure can be applied for other phases. The routine comes to an end when the volume constraints of all constituent phases are satisfied and the objective function converges.

The filtering scheme can effectively alleviate the numerical instabilities of checkerboard pattern and mesh-dependency in the BESO procedure. The filtering is performed by using the following weighting equation [23]:

$$\bar{\alpha}_{\text{in}} = \frac{\sum_{s=1}^{M} w_{\text{is}}\alpha_{\text{in}}}{\sum_{s=1}^{M} w_{\text{is}}} \tag{11}$$

in which $\bar{\alpha}_{\text{in}}$ is the filtered sensitivity number of the ith element for the nth series of sensitivities. The weight factor w_{is} is defined by

$$w_{\text{is}} = \begin{cases} r_{\min} - r_{\text{is}} & \text{if } r_{\text{is}} < r_{\min} \\ 0 & \text{otherwise} \end{cases} \tag{12}$$

where r_{is} denotes the distance between the centers of elements i and s. The filter radius of $r_{\min}$ is defined to identify the neighboring elements that affect the sensitivity of element i. To improve the convergence of the solution, elemental sensitivity numbers can be further averaged with their values in previous iteration [23].

3. Numerical procedure

Taking the design of three-phase composite as an example, the numerical procedure for topology optimization of a multi-phase composite consists of the following steps:

Step 1: Define the BESO parameters such as evolutionary rate ER, filter radius $r_{\min}$, penalty factor p (normally $p = 3$) as well as constituent phases' properties and prescribed volume fractions of the phases V^{1*}, V^{2*} and V^{3*}.
Step 2: Build a finite element model for the PBC in which all elements are assigned with material 1 properties except for some limited number of elements from material 2 as the initial topology.
Step 3: Apply periodic boundary conditions on the PBC and impose uniform strain fields or heat fluxes. Carry out the finite element analysis (FEA) to obtain nodal displacements or temperature fields.
Step 4: Calculate the elemental sensitivity numbers α_{i1} using Eqs. (3) and (6) for maximizing bulk or shear modulus or (4)

and (8) for maximizing thermal conductivity. Calculate α_{i2} if the volume constraint of material 2 has already been satisfied.
Step 5: Filter sensitivity numbers α_{i1}; average α_{i1} with its corresponding value from previous iteration [23].
Step 6: If the prescribed volume of material 2 has already been satisfied, filter the sensitivities α_{i2} and average with its previous values.
Step 7: Determine the target volume for the next iteration. When the current volume $V^k_{(2)}$ is less than the prescribed value V^{2*} (k is the current iteration number), the target volume for the next iteration can be calculated by

$$V^{k+1}_{(2)} = \min\left[V^{2*}, V^k_{(2)}(1+ER)\right] \tag{13a}$$

Step 8: If $V_{(2)} = V^{2*}$ then the volume of material 3 is set as:

$$V^{k+1}_{(3)} = \min\left[V^{3*}, V^k_{(3)}(1+ER)\right] \tag{13b}$$

Step 9: If $V_{(2)} = V^{2*}$ then rank elements based on α_{i2}. Reset elemental densities x_{i2} by changing from 1 (material 2) to $x_{\min}$ (material 3) for elements with lower sensitivities and from $x_{\min}$ to 1 (material 2) for materials with higher sensitivities while satisfying the volume constraint of material 3.
Step 10: Rank elements based on α_{i1}. Reset elemental densities x_{i1} by changing from 1 (material 1) to $x_{\min}$ (material 2) for elements with the lowest sensitivity numbers and from $x_{\min}$ to 1 for elements with the highest sensitivity numbers while satisfying the volume constraint of material 2.
Step 11: Repeat 3–10 until both volume constraints and convergence criterion are satisfied. The convergence criterion is defined in terms of the changes in the objective function (K, G or κ_c) as:

$$\frac{\left|\sum_{i=1}^{\theta}(\phi^{t-i+1} - \phi^{t-N-i+1})\right|}{\sum_{i=1}^{\eta}\phi^{t-i+1}} \le \tau \tag{14}$$

where ϕ is the effective value of the objective function; τ is the prescribed allowable convergence error and θ is the summation upper bound. τ and θ are usually set equal to 0.1% and 5% respectively which means that the convergence is deemed to be attained when the variations of the objective function over the last 10 iterations is equal to or less than 0.1%.

4. Results and discussion

Theoretically, it is possible to derive an approximate admissible range of composite's effective properties. These theoretical relationships are known as bounds. They are derived mainly based on the variational principles and are used for predicting the range of properties that a composite can achieve with a given material composition and volume fractions. They are also extensively used for verification of optimality of designed microstructures through topology optimization [27,28].

For well-ordered, quasi-homogenous and quasi-isotropic composites, the upper and lower bounds on bulk modulus have been derived by Hashin and Shtrikman [29]. As indicated in [14] the Hashin–Shtrikman (HS) bounds on the bulk modulus are not only valid for isotropic materials but also applicable for materials with square symmetry (in 2D cases) and cubic symmetry (in 3D cases) properties; however, such analogy does not exist in the case of shear modulus.

For 2D plane stress cases in which the material consist of three constituent phases, the HS upper bound is given with the following expression [29]:

$$K^{HS}_{\max} = \frac{1}{\frac{f^1}{K^1+G_{\max}} + \frac{f^2}{K^2+G_{\max}} + \frac{f^3}{K^3+G_{\max}}} - G_{\max} \tag{15}$$

and in 3D cases:

$$K^{HS}_{\max} = \frac{1}{\frac{f^1}{K^1+4/3G_{\max}} + \frac{f^2}{K^2+4/3G_{\max}} + \frac{f^3}{K^3+4/3G_{\max}}} - 4/3G_{\max} \tag{16}$$

in which f^1, f^2 and f^3 are the volume fractions of materials 1, 2 and 3 respectively; K^1, K^2 and K^3 are the bulk moduli of constituent phases and $G_{\max}$ is the shear modulus of the strongest material defined as:

$$G_{\max} = E^1/2(1+\nu) \tag{17}$$

Similarly, analytical bounds can be derived for the effective magnetic permeability of macroscopically homogeneous and isotropic multiphase materials [30]. The mathematical analogy enables the results to be used for dielectric, electric conductivity, heat conductivity, and diffusivity of composite materials. It should be noted that in these cases there is no difference between isotropic and square or cubic symmetric materials. The Hashin–Shtrikman upper bound for the thermal conductivity of three-phase 2D isotropic/square symmetric materials is expressed as:

$$\kappa^{HS}_{\max} = -\kappa_{\max} + \frac{1}{\frac{f^1}{\kappa^1+\kappa_{\max}} + \frac{f^2}{\kappa^2+\kappa_{\max}} + \frac{f^3}{\kappa^3+\kappa_{\max}}} \tag{18}$$

in which $\kappa_{\max}$ is the largest eigenvalue of the thermal conductivity of constituent phases.

In 3D cases when the eigenvalues sorted as ($\kappa^1 > \kappa^2 > \kappa^3$), the HS upper bound on the thermal conductivity is:

$$\kappa^{HS}_{\max} = \kappa^1 + \frac{\chi}{1 - \frac{\chi}{3\kappa^1}} \tag{19}$$

in which:

$$\chi = \frac{f^2}{\frac{1}{(\kappa^2-\kappa^1)} + \frac{1}{3\kappa^1}} + \frac{f^3}{\frac{1}{(\kappa^3-\kappa^1)} + \frac{1}{3\kappa^1}} \tag{20}$$

In the following section, some multi-phase composites design examples are presented in which the proposed optimization method is used. The numerical results will be compared with the above theoretical predications.

4.1. 2D three-phase composite with maximum bulk modulus

For designing microstructures of three-phase composites with maximum bulk modulus, the square design domain with dimensions 80×80 is discretized into 80×80, 4-node square elements. The Young's moduli of materials 1, 2 and 3 are selected as $E^1 = 4.0$, $E^2 = 2.0$ and $E^3 = 1.0$ respectively. The Poisson's ratio of all constituent phases is assumed $\upsilon = 0.3$. The evolution rate $ER = 0.02$, filter radius $r_{\min} = 8$ and penalty exponent $p = 3$ are selected as the BESO parameters. The finite element model of the PBC initially consists of elements with material 1 except for four elements of material 2 located at the center of the model. The prescribed volume fractions of materials 1, 2 and 3 are 30%, 40% and 30% respectively.

The final microstructures and the material effective elasticity matrix are given in Fig. 1. The whole procedure converges in 51 iterations for this instance. Fig. 2 presents the evolution histories of bulk modulus, volume fraction and microstructural topology of this example. As it can be seen from the figure, when the procedure starts, the volume of constituent phase 2 is gradually increased. The transition between constituent phases 1 and 2 takes place by ranking the elements based on sensitivity number α_{i1} and satisfying the volume constraint as per Eq. (13a). Once the constituent phase 2 satisfies the prescribed volume fraction (for this example at iteration 24 in Fig. 2), its volume is kept constant. Thereafter, the volume of constituent phase 3 is gradually increased (in Fig. 2, the breakage in bulk modulus' curve at iteration 24 is due to this matter). Transition to constituent phase 3 takes place by

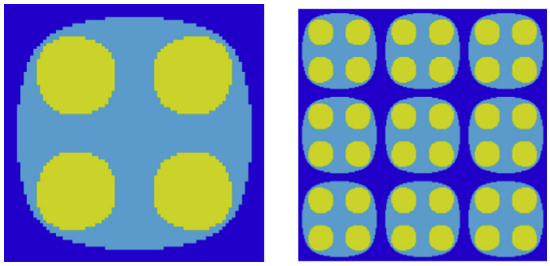

$$\mathbf{D} = 2.214 \begin{bmatrix} 1.0 & 0.275 & 0 \\ 0.275 & 1.0 & 0 \\ 0 & 0 & 0.316 \end{bmatrix}$$

(a) (b) (c)

Fig. 1. 2D 3-phase microstructure of material with maximum bulk modulus (Example 4.1); Material 1 is shown in dark blue (darkest region) ($E^1 = 4$); material 2 in light blue ($E^2 = 2$); and material 3 in yellow (lightest region) ($E^3 = 1$); (a) single base cell; (b) 3×3 cells; (c) elasticity matrix. (For interpretation of the references to colour in this figure legend, the reader is referred to the web version of this article.)

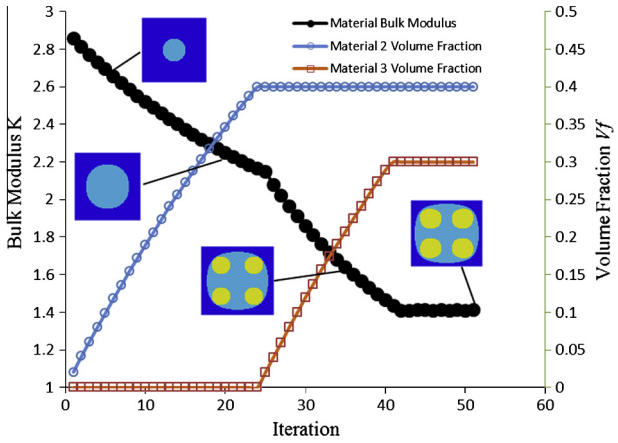

Fig. 2. Evolution histories of bulk modulus, volume fraction and microstructural topology (Example 4.1).

ranking the elements based on sensitivity number α_{i2} and gradually changing the volume of constituent phase 3 as per Eq. (13b). The procedure continues until phase 3 satisfies its prescribed volume fraction and no further improvement happens in the objective function over 10 iterations.

As it can be calculated from the elasticity matrix in Fig. 1, the bulk modulus of the material is 1.411. The Hashin–Shtrikman upper bound is 1.435 from Eq. (15) which shows a good agreement with the obtained result. In comparison with similar problems that have been solved by using the SIMP topology optimization technique [14], the developed procedure indicates certain advantages in terms of computational cost. It is also noticed that the constituent phases of the created microstructures with BESO have distinctive boundaries without "gray areas" which makes the manufacturing easier.

4.2. 3D three-phase composite with maximum bulk modulus

The cubic finite element model with dimensions $40 \times 40 \times 40$ is discretized into $40 \times 40 \times 40$, 8-node cubic elements. As before, mechanical properties of constituent phases are selected as the Young's moduli of $E^1 = 4.0$, $E^2 = 2.0$ and $E^3 = 1.0$ for materials 1, 2 and 3 respectively. The Poisson's ratio of all materials is $v = 0.3$. The evolution rate $ER = 0.02$, filter radius $r_{min} = 2$ and penalty exponent $p = 3$ are selected as the BESO parameters. The initial material distribution in the finite element model of the PBC consists of all elements with material 1 properties, except for eight elements at the center and eight elements at the eight corners with material 2. The prescribed volume fraction of materials 1, 2 and 3 are 30%, 50% and 20% respectively.

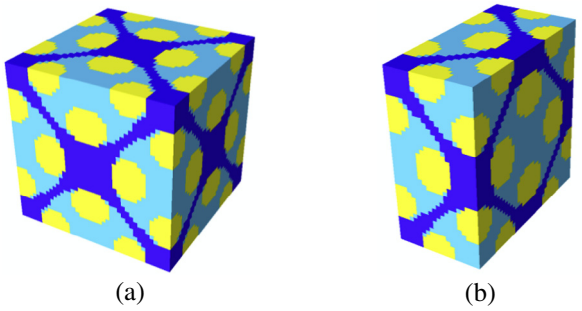

(a) (b)

$$\mathbf{D} = 2.902 \begin{bmatrix} 1 & 0.421 & 0.421 & 0 & 0 & 0 \\ 0.421 & 1 & 0.421 & 0 & 0 & 0 \\ 0.421 & 0.421 & 1 & 0 & 0 & 0 \\ 0 & 0 & 0 & 0.296 & 0 & 0 \\ 0 & 0 & 0 & 0 & 0.296 & 0 \\ 0 & 0 & 0 & 0 & 0 & 0.296 \end{bmatrix} \quad \text{(c)}$$

Fig. 3. 3D 3-phase microstructure of material with maximum bulk modulus (Example 4.2). Material 1 is shown in dark blue (darkest region) ($E^1 = 4$); material 2 in light blue ($E^2 = 2$); and material 3 in yellow (lightest region) ($E^3 = 1$); (a) single base cell; (b) middle-cut of the cell; (c) elasticity matrix of corresponding material. (For interpretation of the references to colour in this figure legend, the reader is referred to the web version of this article.)

The final microstructures and the material effective elasticity matrix are given in Fig. 3 with the bulk modulus 1.782. The HS upper bound for the setting of this example is 1.801 from Eq. (16), which is very close to the obtained result. The whole BESO procedure only needs 53 iterations. Fig. 4 demonstrates the evolution histories of bulk modulus, volume fraction and microstructural topology of this example.

4.3. 2D three-phase composite with maximum shear modulus

The objective of this example is the topology optimization of microstructures to achieve composite with maximum average shear modulus along principal directions. The prescribed volume fraction of constituent phases 1, 2 and 3 are selected 30%, 40% and 30% of the total volume respectively. The 2D square design domain with dimensions 80×80 is discretized into 80×80, 4-node square elements. The mechanical properties of the 3 constituent phases are selected similar to the previous example. The evolution rate of $ER = 0.02$, filter radius $r_{min} = 8$ and penalty exponent $p = 3$ are selected as the BESO initial parameters. In the initial finite element model of the PBC, material 1 property is assigned to all elements except for four elements of material 2 at the center of

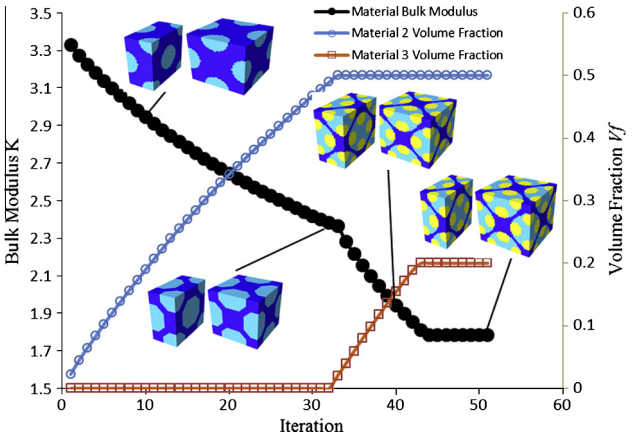

Fig. 4. Evolution histories of bulk modulus, volume fraction and microstructural topology (Example 4.2).

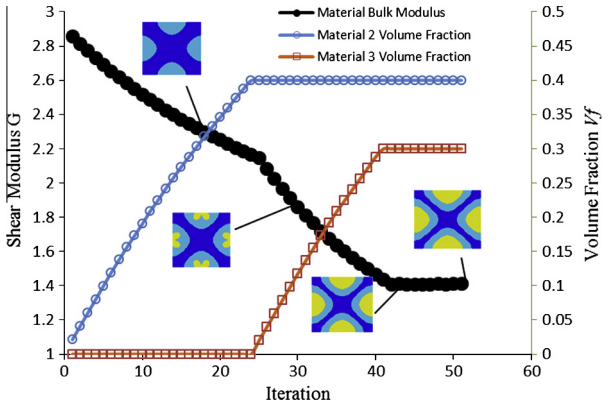

Fig. 6. Evolution histories of shear modulus, volume fraction and microstructural topology (Example 4.3).

the design domain. The generated microstructures as well as the material effective elasticity matrix are shown in Fig. 5. Fig. 6 demonstrates the evolution histories of shear modulus and volume fraction of the generated microstructure throughout the optimization process. The procedure converges to the final topology after 51 iterations. The generated microstructure is comparable with the cellular materials which are optimized with similar objective function in literature [31,32].

4.4. 3D three-phase composite with maximum shear modulus

For the design of three-phase microstructure of material with maximum shear modulus, a cubic design domain with dimensions $24 \times 24 \times 24$ is discretized into $24 \times 24 \times 24$, 8-node cubic elements. As before, the Young's moduli of constituent phases are selected as $E^1 = 4.0$, $E^2 = 2.0$ and $E^3 = 1.0$; the Poisson's ratio is assumed $v = 0.3$ for all three phases. The BESO parameters are the evolution rate $ER = 0.02$, filter radius $r_{\min} = 2$ and penalty exponent $p = 3$. The prescribed volume fraction of materials 1, 2 and 3 are 25%, 45% and 30% respectively. The initial material distribution in the finite element model consists of elements, all with phase 1 properties, except for four elements of material 2 at the center of the design domain.

The resulted microstructural topology is shown in Fig. 7; the figure also demonstrates the spatial distribution of each constituent phase as well as the homogenized effective elasticity matrix of material. Fig. 8 demonstrates the evolution histories of shear modulus and volume fraction of the designed microstructure throughout the iterative process. It can be seen from the figure, the procedure converges to the final topology after 56 iterations.

4.5. 2D three-phase composite with maximum thermal conductivity

To demonstrate the efficiency of the algorithm for the topology optimization of materials with maximum thermal conductivity, the square design domain of the PBC with dimensions 80×80 is discretized into 80×80, 4-node quadrilateral elements. The thermal conductivities of materials 1, 2 and 3 are selected as $\kappa^1 = 4.0$, $\kappa^2 = 2.0$ and $\kappa^3 = 1.0$ respectively. The BESO parameters are set as the evolution rate $ER = 0.02$, filter radius $r_{\min} = 8$ and penalty exponent $p = 3$. The initial finite element model of the PBC consists of elements with constituent phase 1 except for four elements of material 2 at the center of the design domain. The prescribed volume fraction of materials 1, 2 and 3 are 25%, 25% and 50% respectively.

The final microstructures and the material homogenized thermal conductivity matrix are given in Fig. 9. With the help of the Eq. (18) the HS upper bound $\kappa^{HS}_{\max}$ is calculated equal to 1.783, whereas the thermal conductivity of generated material is 1.764 (from the material matrix in Fig. 8). For three-phase materials, it is shown theoretically that the HS upper bound can be attained precisely, if $\kappa^{HS}_{\max} \geqslant \kappa^2$ [14,33].

The whole procedure completes in 29 iterations. Fig. 10 demonstrates the evolution histories of thermal conductivity, volume fraction and microstructural topology of this example. The above results are comparable with the microstructures generated by the SIMP method in [18]. Topology optimization of 2D microstructures with the SIMP procedure typically needs between 60 and 100 iterations to converge [18]. It should be mentioned that the topology optimization of microstructures for materials have not a unique solution and there are many local optima. The resulted microstructures are dependent on factors such as the applied optimization algorithm and the design parameters.

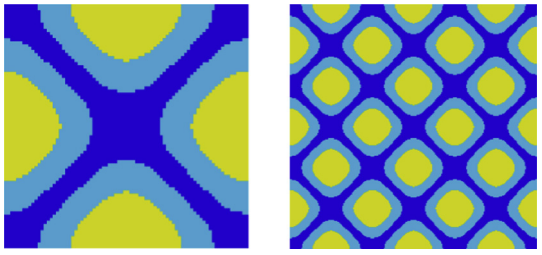

(a) (b)

$$\mathbf{D} = 2.105 \begin{bmatrix} 1.0 & 0.342 & 0 \\ 0.342 & 1.0 & 0 \\ 0 & 0 & 0.385 \end{bmatrix}$$

(c)

Fig. 5. 2D 3-phase microstructure of material with maximum shear modulus (Example 4.3). Material 1 is shown in dark blue (darkest region) ($E^1 = 4$); material 2 in light blue ($E^2 = 2$); and material 3 in yellow (lightest region) ($E^3 = 1$); (a) single base cell; (b) 3×3 cells; (c) elasticity matrix. (For interpretation of the references to colour in this figure legend, the reader is referred to the web version of this article.)

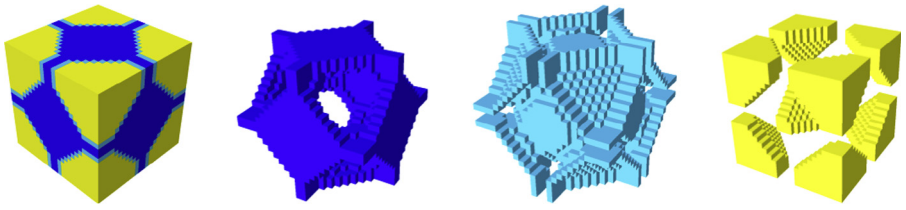

$$\mathbf{D} = 2.624 \begin{bmatrix} 1 & 0.412 & 0.412 & 0 & 0 & 0 \\ 0.412 & 1 & 0.412 & 0 & 0 & 0 \\ 0.412 & 0.412 & 1 & 0 & 0 & 0 \\ 0 & 0 & 0 & 0.298 & 0 & 0 \\ 0 & 0 & 0 & 0 & 0.298 & 0 \\ 0 & 0 & 0 & 0 & 0 & 0.298 \end{bmatrix} \quad \text{(e)}$$

Fig. 7. 3D 3-phase microstructure of material with maximum shear modulus (Example 4.4); (a) single base cell; (b) topology of constituent phase 1 ($E^1 = 4$); (c) topology of constituent phase 2 ($E^2 = 2$); (d) topology of constituent phase 3 ($E^3 = 1$); (e) elasticity matrix of material.

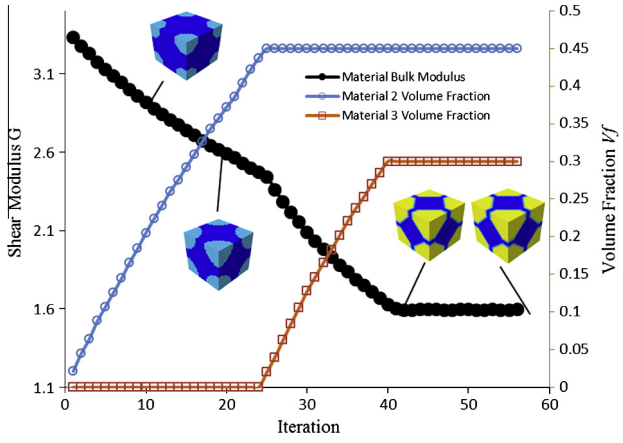

Fig. 8. Evolution histories of shear modulus, volume fraction and microstructural topology (Example 4.4).

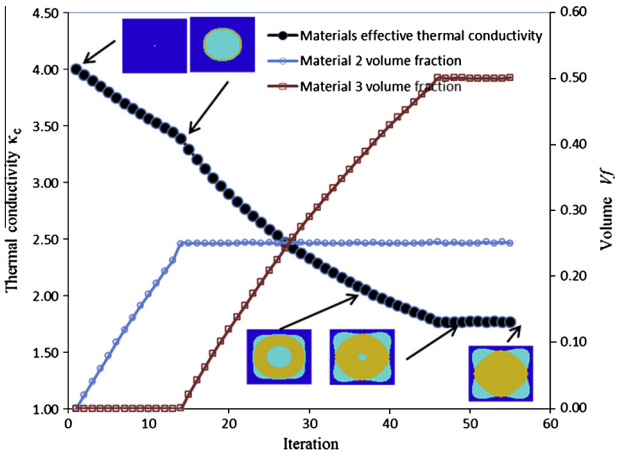

Fig. 10. Evolution histories of thermal conductivity, volume fraction and microstructural topology (Example 4.5).

4.6. 3D three-phase composite with maximum thermal conductivity

The objective of this example is to design 3D microstructures for materials with maximum thermal conductivity. The PBC with dimensions $42 \times 42 \times 42$ is discretized into $42 \times 42 \times 42$, eight-node cubic finite elements. As before the eigenvalues of thermal conductivity of constituent materials 1, 2 and 3 are selected as 4, 2 and 1 respectively. The BESO parameters are evolution rate $ER = 0.02$ and the filter radius $r_{min} = 3$. The procedure starts from the initial design in which all elements are assigned with material 1 property except for 4 elements of material 2 at the center of the finite element model. The prescribed volume fraction of the materials 1, 2 and 3 are 25%, 25% and 50% respectively.

Fig. 11 shows the resulting microstructures and the thermal conductivity matrix of material. The HS upper bound from the Eq. (19) is calculated equal to 1.863 which shows 0.7% difference with the designed microstructure (1.849 in Fig. 11). Fig. 12 shows the evolution histories of thermal conductivity, volume fraction and microstructural topology of this example.

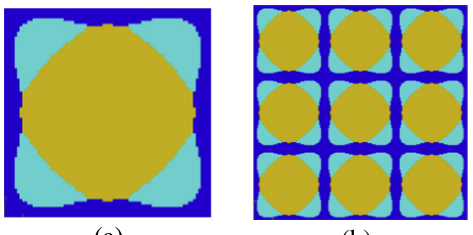

$$\boldsymbol{\kappa} = \begin{bmatrix} 1.764476 & 0 \\ 0 & 1.764476 \end{bmatrix} \quad \text{(c)}$$

Fig. 9. 2D 3-phase microstructure of material with maximum thermal conductivity (Example 4.5). Material 1 is shown in dark blue (darkest region) ($\kappa^1 = 4$); material 2 in light blue ($\kappa^2 = 2$); and material 3 in yellow (lightest region) ($\kappa^3 = 1$); (a) single base cell; (b) 3×3 cells; (c) matrix if thermal conductivity. (For interpretation of the references to colour in this figure legend, the reader is referred to the web version of this article.)

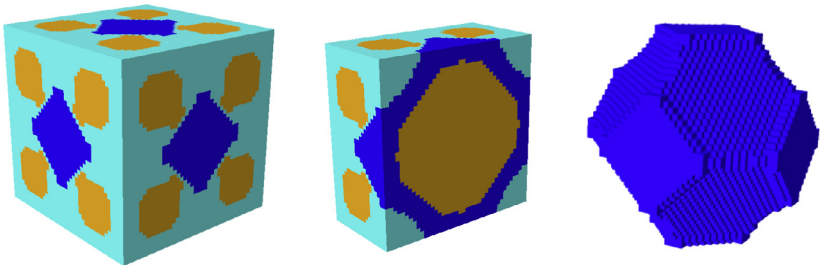

$$\boldsymbol{\kappa} = \begin{bmatrix} 1.84911 & 0 & 0 \\ 0 & 1.84911 & 0 \\ 0 & 0 & 1.84911 \end{bmatrix} \quad \text{(d)}$$

Fig. 11. 3D 3-phase microstructure of material with maximum thermal conductivity (Example 4.6). Material 1 is shown in dark blue (darkest region) ($\kappa^1 = 4$); material 2 in light blue ($\kappa^2 = 2$); and material 3 in yellow (lightest region) ($\kappa^3 = 1$); (a) single base cell; (b) middle-cut of the cell; (c) spatial distribution of material 1; (d) thermal conductivity matrix. (For interpretation of the references to colour in this figure legend, the reader is referred to the web version of this article.)

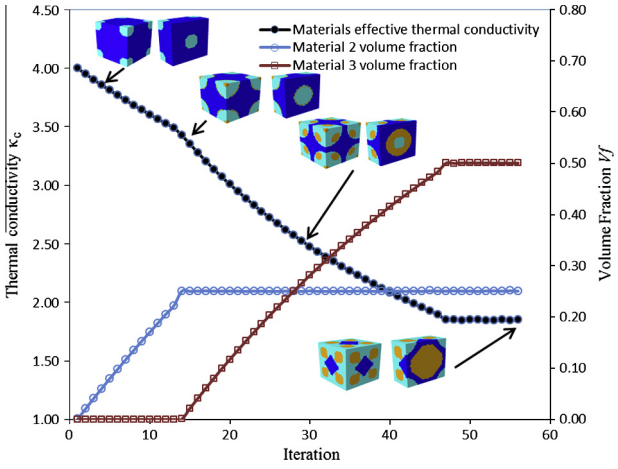

Fig. 12. Evolution histories of thermal conductivity, volume fraction and microstructural topology (Example 4.6).

5. Conclusion

The BESO method has been extended to the design of multi-phase microstructures of composite materials for maximum bulk modulus, shear modulus or thermal conductivity. The numerical examples demonstrate that the proposed approach is capable of generating composite microstructures with properties very close to known analytical bounds. The evolution histories of volume fraction and microstructure topology show that the proposed method can successfully obtain convergent solutions with high computational efficiency. Moreover, as an inherent property of the BESO, there are distinctive interfaces between constituent phases in the generated microstructures which make the manufacturing of generated materials straightforward.

Multi-functional materials are inevitably composites of two or more constituent phases [1]. The methodology presented here can be extended to the design of multi-phase materials with multi-objective functions, as illustrated for two non-zero phase materials with variation in stiffness and thermal conductivity in [34].

References

[1] R.F. Gibson, Compos. Struct. 92 (2010) 2793–2810.
[2] O. Sigmund, Int. J. Solids Struct. 31 (17) (1994) 2313–2329.
[3] O. Sigmund, Mech. Mater. 20 (4) (1995) 351–368.
[4] S. Osher, J.A. Sethian, J. Comput. Phys. 79 (1) (1988) 12–49.
[5] S. Zhou, M.Y. Wang, Struct. Multidiscip. Opt. 33 (2) (2007) 89–111.
[6] X. Wang, M.Y. Wang, D. Guo, Struct. Multidiscip. Opt. 27 (1–2) (2004) 1–19.
[7] M. Burger, B. Hackl, W. Ring, J. Comput. Phys. 194 (1) (2004) 344–362.
[8] M.P. Bendsøe, N. Kikuchi, Comput. Methods Appl. Mech. Eng. 71 (2) (1988) 197–224.
[9] K. Terada, N. Kikuchi, Mater. Sci. Res. Int. 2 (2) (1996) 65–72.
[10] D. Fujii, B.C. Chen, N. Kikuchi, Int. J. Numer. Meth. Eng. 50 (9) (2001) 2031–2051.
[11] M.P. Bendsøe, O. Sigmund, Arch. Appl. Mech. 69 (9) (1999) 635–654.
[12] G.I.N. Rozvany, M. Zhou, T. Birker, Struct. Multidiscip. Opt. 4 (3) (1992) 250–252.
[13] O. Sigmund, S. Torquato, J. Mech. Phys. Solids 45 (6) (1997) 1037–1067.
[14] L.V. Gibiansky, O. Sigmund, J. Mech. Phys. Solids 48 (3) (2000) 461–498.
[15] O. Sigmund, J. Petersson, Struct. Opt. 16 (1) (1998) 68–75.
[16] C.C. Swan, I. Kosaka, Int. J. Numer. Meth. Eng. 40 (1997) 3033–3057.
[17] L. Yin, W. Yang, Comput. Struct. 79 (20–21) (2001) 1839–1850.
[18] S. Zhou, Q. Li, Comput. Mater. Sci. 43 (3) (2008) 549–564.
[19] S. Zhou, M. Wang, Struct. Multidiscip. Opt. 33 (2) (2007) 89–111.
[20] J.K. Guest, J.H. Prévost, T. Belytschko, Int. J. Numer. Meth. Eng. 61 (2) (2004) 238–254.
[21] M.Y. Wang, S. Zhou, H. Ding, Struct. Multidiscip. Opt. 28 (4) (2004) 262–276.
[22] X. Huang, Y.M. Xie, Comput. Mech. 43 (3) (2009) 393–401.
[23] X. Huang, Y.M. Xie, Evolutionary Topology Optimization of Continuum Structures: Methods and Applications, John Wiley & Sons Ltd., 2010.
[24] B. Hassani, E. Hinton, Comput. Struct. 69 (6) (1998) 707–717.
[25] B. Hassani, E. Hinton, Comput. Struct. 69 (6) (1998) 719–738.
[26] E.J. Haug, K.K. Choi, V. Komkov, Design Sensitivity Analysis of Structural Systems, Academic Press, Orlando, 1986.
[27] J. Cadman, S. Zhou, Y. Chen, Q. Li, J. Mater. Sci. 48 (1) (2013) 51–66.
[28] V.J. Challis, A.P. Roberts, A.H. Wilkins, Int. J. Solids Struct. 45 (14–15) (2008) 4130–4146.
[29] Z. Hashin, S. Shtrikman, J. Mech. Phys. Solids 11 (2) (1963) 127–140.
[30] Z. Hashin, S. Shtrikman, J. Appl. Phys. 33 (10) (1962) 3125–3131.
[31] X. Huang, A. Radman, Y.M. Xie, Comput. Mater. Sci. 50 (6) (2011) 1861–1870.
[32] M.M. Neves, H. Rodrigues, J.M. Guedes, Comput. Struct. 76 (2000) 421–429.
[33] S. Zhou, Q. Li, J. Mater. Res. 23 (03) (2008) 798–811.
[34] A. Radman, X. Huang, Y.M. Xie, Comput. Mater. Sci. 82 (2014) 457–463.